J|A|C|S
COMMUNICATIONS

Published on Web 05/25/2007

Doubly Ortho-Linked *cis*-4,4′-Bis(diarylamino)stilbene/Fluorene Hybrids as Efficient Nondoped, Sky-Blue Fluorescent Materials for Optoelectronic Applications

Yi Wei and Chien-Tien Chen*

Department of Chemistry, National Taiwan Normal University, Taipei, Taiwan 11650

Received February 5, 2007; E-mail: chefv043@ntnu.edu.tw

There has been great interest in developing electroluminescent molecular materials with sharp and bright blue emissions for organic light emitting diodes (OLEDs) in flat-panel display in recent years.[1] Several efficient UV molecular host materials integrated with suitable blue-emitting dopants have been developed with pending stability issues during prolonged operation.[2] Conversely, many researchers have tried to come up with ultimate, nondoped hosts by utilizing the derivatives of bistriphenylenyl,[3] diarylfluorene/spirobifluorene,[4] and diarylanthracene.[5]

trans-4,4′-Bis(diarylamino)stilbene derivatives are generally adopted as blue fluorescent materials.[6] However, their ready trans to cis photoisomerization profiles and close interchromophoric contact significantly reduce their emission efficiency both in solution and in the solid state, limiting their extensive applications in OLED.[7] To prevent the radiationless photoisomerization through the confinement of the *cis*-stilbene configuration in a cyclic framework, we sought a new concept of this type by affixing the two individual ortho-positions of the phenyl rings in *cis*-stilbene onto the C-9 position of fluorene (Scheme 1). The resultant spirally connected, butterfly-shaped framework[8] can avoid intimate intermolecular chromophoric $\pi-\pi$ stacking responsible for emission quenching or shifting due to eximer formation. By appending two hole-transporting diarylamino segments onto both para positions of the *cis*-stilbene template, sky-blue fluorescent OLED materials can be furnished with high EL brightness and working efficiencies. Herein, we report the preliminary result toward this end.

The target molecules **5a**−**c** can be synthesized in three steps from 3,7-dibromo-dibenzosuberenone-**3** by treatment with 2-lithiobiphenyl and subsequent intramolecular Friedel−Crafts alkylation of the resulting 3° alcohol and final coupling with diarylamines.[9] The structural features of **5a**−**c** were determined by NMR spectroscopic and X-ray crystallographic analysis. As represented in **5c**, it exists as a dimer in unit cell with planar nitrogen units ($\Sigma\angle = 359 \pm 0.6°$),[9] Figure 1. Both the flanking diarylamino units are tilted by 28−38° relative to the central dibenzosuberene (DBE) template. The 4-methoxyphenyl units are tilted by 27.4 ± 0.9° and 58.4 ± 2.8°, respectively. The rigid butterfly-shaped structure with a spiral tail not only prevents facile conformational flipping of the central 7-membered ring in the DBE core but also avoids intermolecular parallel $\pi-\pi$ stacking.

Upon UV excitation, **5a**−**c** show similar blue emission color with emission maxima in the range of 454−483 nm with quantum yields up to 90%. The full-width at half-maximum (fwhm) for each individual emission ranges from 53 to 60 nm, which may act as ideal sky-blue emitters particularly for **5a** and **5b** (Table 1). Conversely, the rigid spiral framework also helps to increase their thermal stability (T_d, 441−473 °C) and glassy transition temperature (T_g, 117−137 °C). In comparison, the T_d (443 °C) for **5a** is 34 and 46 °C higher than those of the corresponding open-form and methylene-linked systems **6** and **8**, respectively (Table 1). Conversely, the T_g (123 °C) for **5a** is 73 and 22 °C higher than those of **6** and **8**, respectively.

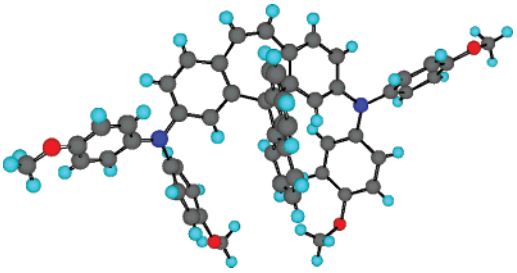

Figure 1. Chem-3D presentation for the X-ray crystal structure of **5c**.

Scheme 1. The Assembly Concept of the *cis*-4,4′-Bis(*N*,*N*-diarylamino)stilbene/Fluorene Optoelectronic System

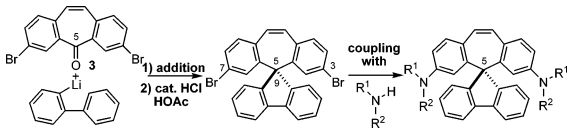

Table 1. Optical, Morphological, and Electrochemical Data for **5a**−**c**, **6**, and **8**

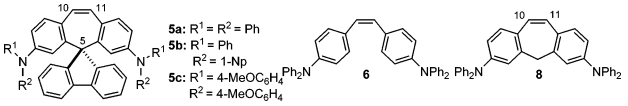

compd	absolute $\lambda_{max}(\epsilon)^a$ nm	$\lambda_{max}{}^a$ nm	$\Phi_f{}^a$ %	T_g/T_d °C	$E_{ox}{}^a$ V
5a	306 (22.2)	461 (57[b])	90	123/443	+0.15
	349 (12.3)				
	406 (23.6)				+0.32
5b	265 (44.5)	454 (53)	58	137/473	+0.15
	347 (26.4)				
	403 (33.0)				+0.36
5c	302 (30.5)	483 (60)	90	117/441	+0.19
	370 (16.6)				
	414 (27.5)				+0.34
6	307 (15.9)	441 (58)	99	50/409	+0.26
	370 (10.4)				
8	306 (22.9)	440 (62)	99	101/397	+0.34
	370 (23.0)				
					+0.71

[a] $\epsilon \times 10^{-3}$; measured in CH_2Cl_2. [b] The data in parentheses correspond to full-width at half-maximum (fwhm).

The redox behaviors of **5a**−**c** were evaluated by cyclic voltammetry (CV) experiments at ambient temperature with Ag/AgCl as a reference electrode. All of these show similar, paired oxidation potentials with reversible redox couples at +0.17 ± 0.02 and +0.34 ± 0.02 V owing to sequential oxidations of the two diarylamino appendages. In marked contrast, the corresponding open-form and

10.1021/ja070822x CCC: $37.00

Table 2. Electroluminescence Data for **5a**−**c**, **6**, and **8**

configuration[a]	Em. λ_{max}	V_{on}, V	η_{ext}[c]	η_c/η_p[c]	L_{max},[d] cd/m^2
5a/**A**	462 (47[b])	2.9 (4.3[c])	1.94	2.9/2.1	11313 (595[c])
5a/**B**	466 (60)	2.8 (5.2)	7.87	13.6/8.2	17609 (2689)
5b/**A**	458 (49)	2.8 (4.0)	3.44	5.4/4.2	14690 (1071)
5b/**B**	462 (52)	2.7 (4.6)	6.35	10.2/6.9	17599 (2034)
5c/**A**	480 (59)	2.5 (3.6)	3.26	7.4/6.5	13615[e] (1454)
5c/**B**	484 (77)	2.5 (4.4)	5.19	12.1/8.6	13806 (2423)
6/**A**	464 (47)	4.6 (8.6)	1.12	1.6/0.6	1223 (319)
8/**A**	468 (70)	3.2 (4.3)	2.42	3.0/1.9	8939 (621)

[a] Configuration **A:** ITO/**5a**−**c**, **6**, or **8** (40 nm)/TPBI(40 nm)/LiF(1 nm)/Al; configuration **B:** ITO/PEDOT:PSS(20 nm)/**5a**−**c**(40 nm)/TPBI (40 nm)/LiF(1 nm)/Al. [b] The data in parentheses correspond to full-width at half-maximum (fwhm). [c] V_{on}, η_{ext} (%), η_c (cd/A), η_p (lm/W), and L_{20} measured at 20 mA/cm^2. [d] At 10.5 V. [e] At 8.5 V.

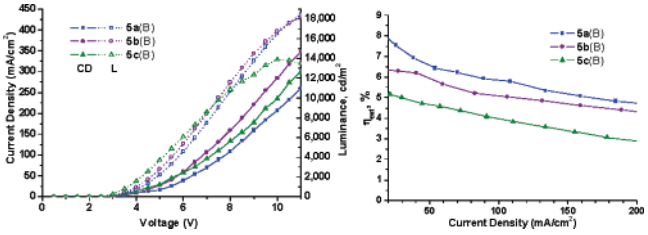

Figure 2. The stacked plots of the $I-V-L$ and $I-\eta_{ext}$ characteristics of devices-**B** for **5a**−**c**.

methylene-linked systems **6** and **8** exhibit only one reversible, two-electron oxidation, redox couple at +0.26 and +0.34 V, respectively. Therefore, the current spiral design shows lower first oxidation potential, which may facilitate better hole injection from ITO to these materials in OLED devices. The second oxidation potential at +0.71 V for **8** is due to facile oxidation at the C(5)-position of the central DBE template.

Their optoelectronic performances were assessed by fabricating **5a**−**c** as an individual hole transport-type emitting layer (40 nm thickness) and making it into a bilayer OLED device configuration-**A** by using 1,3,5-*tris*-(*N*-phenyl-benzimidazole-2-yl)benzene (TBPI; 40 nm thickness)[10a] as the electron-transport (ET) layer (Table 2). The resultant OLED devices exhibit EL brightness (L_{max}) values of 11313, 14690, and 13615 cd/m^2, respectively, at 8.5 or 10.5 V.[9] Their operational brightness (L_{20}) at 20 mA/cm^2 can reach 595, 1071, and 1454 cd/m^2, respectively, with individual external quantum efficiencies (η_{ext}) of 1.9, 3.4, and 3.3%. Their luminance and power efficiencies (η_c/η_p) are 2.9/2.1, 5.4/4.2, and 7.4/6.5 cdA^{-1}/lmW^{-1}, respectively. Notably, the device performances from these spirally shaped materials **5a**−**c** are at least two times better than those of the corresponding open form systems as represented by **6** (L_{max} 1223 cd/m^2) in all aspects. On the other hand, the devices-**A** from both **5a** and **8** are equally efficient except with lower L_{max} (8939 cd/m^2) and broader emission (70 nm) for **8** presumably due to the flexible nature of **8** which lacks the spirally linked fluorene damper of **5a**. Therefore the preliminary results support the concept of our new molecular design. To optimize their device efficiency, PEDOT/PSS[10b] was chosen as a hole-injection layer (20 nm thickness) along with TPBI as the ET layer as in device configuration-**B**. It was found that PEDOT/PSS significantly facilitates the injection of holes from the ITO anode into the HT-type emitting materials **5a**−**c**. These devices in configuration-**B** exhibit an L_{max} of 17609, 17599, and 13806 cd/m^2, respectively, at 10.5 V.[9] Their L_{20} values reach 2689, 2034, and 2423 cd/m^2, respectively, with individual external quantum efficiencies (η_{ext}) of 7.9, 6.4, and 5.2% (Figure 2). Their η_c/η_pvalues are 13.6/8.2, 10.2/6.9, 12.1/8.6 cdA^{-1}/lmW^{-1}, respectively. Overall, their external quantum efficiency, operational brightness, and operational efficiency in configuration-**B** were improved by about 4 times for **5a** and by 1.7−1.9 times for **5b** and **5c**, albeit with slightly higher operational voltages by 0.6−0.9 V. Conversely, when 2,9-dimethyl-4,7-diphenyl-1,10-phenanthroline (BCP[10c]) was used to replace TPBI in device-**B**, the resulting device-**C** operated 75% as efficient.[9]

Notably, the external quantum efficiencies (η_{ext}) in device configuration-**B** for **5a**,**b** are approaching or greater than the theoretical maximum of about 6.5% for common fluorescent-type molecular materials. A recent report by Fujihira suggested that extra singlet excited-state formation may be facilitated through triplet−triplet annihilation of a given triplet excited state, which attributes to an additional fluorescent emission by 60% of the original maximum (i.e., corrected max for η_{ext} is 10.4%).[11] The unprecedented high external quantum efficiency (η_{ext}, 7.9%) exhibited by **5a** in device configuration-**B** indicates potential facile triplet−triplet annihilation of **5a** with enhanced singlet-state formation in the cyclic DBE skeleton by placing the triplet biradical at both pseudoaxial positions of C10 and C11. The pseudoaxially disposed triplet biradical can thus be readily transformed back to the corresponding singlet biradical through conjugation with both the diarylamino moieties. To our knowledge, blue-emitting **5a** represents one of the best blue fluorescent materials to date, and its optoelectronic performance is also somewhat comparable to some doped phosphorescent devices.[12] Particularly, saturated sky-blue OLED device-**B** [CIE (x,y):(0.15,0.25)] resulted well from **5a** augur for its further applications in full-color display technology.

Acknowledgment. We thank the National Science Council of Taiwan for generous financial support of this research.

Supporting Information Available: Experimental, device, and spectra details of **2**−**5**, **6**, and **8** and cif file for **5c**. This material is available free of charge via the Internet at http://pubs.acs.org.

References

(1) (a) Mullen, K.; Scherf, U.; *Organic Light-Emitting Devices. Synthesis, Properties and Applications;* Wiley: Weinheim, Germany, 2006. (b) Burroughes, J. H.; Bradley, D. D. C.; Brown, A. R.; Marks, R. N.; Mackay, K.; Friend, R. H.; Burns, P. L.; Holmes, A. B. *Nature* **1990**, *347*, 539.
(2) Gong, J.-R.; Wan, L.-J.; Lei, S.-B.; Bai, C.-L.; Zhang, X.-H.; Lee, S.-T. *J. Phys. Chem. B* **2005**, *109*, 1675.
(3) Shih, H.-T.; Lin, C.-H.; Shih, H.-H.; Cheng, C.-H. *Adv. Mater.* **2002**, *14*, 1409.
(4) (a) Wu, C.-C.; Lin, Y.-T.; Chiang, H.-H.; Cho, T.-Y.; Chen, C.-W.; Wong, K.-T.; Liao, Y.-L.; Lee, G.-H.; Peng, S.-M. *Appl. Phys. Lett.* **2002**, *81*, 577. (b) Tao, S.; Peng, Z.; Zhang, X.; Wang, P.; Lee, C.-S.; Lee, S.-T. *Adv. Funct. Mater.* **2005**, *15*, 1716. (c) Tang, C.; Liu, F.; Xia, Y.-J.; Lin, J.; Xie, L.-H.; Zhong, G.-Y.; Fan, Q.-L.; Huang, W. *Org. Electron.* **2006**, *7*, 155.
(5) Tao, S.; Hong, Z.; Peng, Z.; Ju, W.; Zhang, X.; Wang, P.; Wu, S.; Lee, S. *Chem. Phys. Lett.* **2004**, *397*, 1.
(6) (a) Rumi, M.; Ehrlich, J. E.; Heikal, A. A.; Perry, J. W.; Barlow, S.; Hu, Z.; McCord-Maughon, D.; Parker, T. C.; Röckel, H.; Thayumanavan, S.; Marder, S. R.; Beljonne, D.; Brédas, J.-L. *J. Am. Chem. Soc.* **2000**, *122*, 9500. (b) Yang, J.-S.; Liau, K.-L.; Wang, C.-M.; Hwang, C.-Y. *J. Am. Chem. Soc.* **2004**, *126*, 12325.
(7) (a) Hosokawa, C.; Higashi, H.; Nakamura, H.; Kusumoto, T. *Appl. Phys. Lett.* **1995**, *67*, 3853. (b) Woo, H.-S.; Cho, S.; Kwon, T.-W.; Park, D.-K. *J. Korean Phys. Soc.* **2005**, *46*, 981.
(8) For the uses of the template in catalysis, LC optical switches, and fluorescent OLED chameleons, see: (a) Chen, C.-T.; Chao, S.-D.; Yen, K.-C.; Chen, C.-H.; Chou, I.-C.; Hon, S.-W. *J. Am. Chem. Soc.* **1997**, *119*, 11341. (b) Chen, C.-T.; Chou, Y.-C. *J. Am. Chem. Soc.* **2000**, *122*, 7662. (c) Chen, C.-T.; Wei, Y.; Lin, J.-S.; Moturu, M. V. R. K.; Chao, W.-S.; Tao, Y.-T.; Chien, C.-H. *J. Am. Chem. Soc.* **2006**, *128*, 10992.
(9) See the Supporting Information for details and for the synthesis of **3**.
(10) (a) Shi, J.; Tang, C.-W.; Chen, C.-H. U.S. Patent 5,645,948, 1997. (b) Elschner, A.; Bruder, F.; Heuer, H.-W.; Jonas, F.; Karbach, A.; Kirchmeyer, S.; Thurm, S.; Wehrmann, R. *Synth. Met.* **2000**, *111*, 139. (c) Yasuda, T.; Yamaguchi, Y.; Zou, D.-C.; Tsutsui, T. *Jpn. J. Appl. Phys.* **2002**, *41*, 5626.
(11) Ganzorig, C.; Fujihira, M. *Appl. Phys. Lett.* **2002**, *81*, 3137.
(12) (a) Ren, X.; Li, J.; Holmes, R. J.; Djurovich, P. I.; Forrest, S. R.; Thompson, M. E. *Chem. Mater.* **2004**, *16*, 4743. (b) Yeh, S.-J.; Wu, M-F.; Chen, C.-T.; Song, Y.-H.; Chi, Y.; Ho, M.-H.; Hsu, S.-F.; Chen, C.-H. *Adv. Mater.* **2005**, *17*, 285.

JA070822X